Illumination Map Smoothing (IMS): A Convex and Differentiable Mathematical Model to Rapidly Enhance Low-Light Images

Abstract:

Automatically retrieving information from images recorded in a low-light environment is a practical challenge for computer vision domain. So far, different mathematical models based on Retinex theory have been proposed to enhance low-light images. Differentiability of the objective function has received less attention in these models. This paper presents a differentiability mathematical model and convex with linear constraints that can provide a chance to acquire global optimum solution. The proposed mathematical model seeks to enhance the visual quality of recovered images via smoothing the initial illumination map. Furthermore, proposed method corrects the illumination map using a simple linear transformation to increase the contrast and readability of enhanced images. This paper also presents a heuristic approach to fast solve the proposed mathematical model with acceptable accuracy. Heuristic approach could be used for image processing applications that low-light images must be enhanced with no noticeable delay. To evaluate, the proposed method is compared with six other competitive methods using six quantitative metrics as well as time cost. The results show that proposed method outperforms other methods and can be used in real-time applications.

Keywords: Low-light Image Enhancement; Retinex theory; Illumination Estimation; Illumination map; Mathematical model

1. Introduction

Algorithms such as object detection [1][2], tracking [3][4][5], scene understanding [6] and occlusion detection [7] are mainly designed for high quality and clear images. The use of low-quality and low-light images can challenge the performance of these algorithms. One of the important factors and affecting the visual quality of images is the lighting of the shooting environment. Images recorded in low-light environment often have low illumination and contrast. In such images, some details of the target scenes are not well recognizable. Therefore, having sufficient and appropriate light in the imaging environment is crucial. However, in some cases, proper lighting is not possible in the shooting environment, such as [8]:

- Intelligence, reconnaissance and surveillance missions (e.g., recognizing and distinguishing enemy warships and identify military bases).
- Shooting in adverse weather conditions (e.g., taking photos in fog and night).
- Unmanned vehicles (e.g., automatic landing of UAVs).

- Commercial industries (e.g., property security, personal mobile phone and surveillance cameras).

Therefore, enhancing low-light images and revealing lost details are important. So, in practice, illumination of low-light images must be improved before applying computer vision techniques in order to ameliorate readability of these images.

Generally, in the literature, the introduced methods for enhancing low-light images can be divided into four categories [9]:

I. Gray Transformation (GT) methods.
II. Histogram Equalization (HE) methods.
III. Machine learning methods.
IV. Retinex theory methods.

In table 1 categorizes some of the research done to enhance low-light images.

Table 1: Some research on enhancing low-light images

Authors	Year	Method type						
		GT	HE		Machine learning	Retinex		
			GHE	LHE		Reflection	Illumination	Noise
Chiu et al.[10]	2011	✓						
Huang et al. [11]	2012	✓						
Huang et al. [12]	2016	✓						
Srinivas et al. [13]	2019	✓						
Kim [14]	1977		✓					
Der Chen et al. [15]	2003		✓					
Wang and Ward [16]	2007		✓					
Kim et al. [17]	1988			✓				
Reza [18]	2004			✓				
Liu et al. [19]	2011			✓				
Lore et al. [8]	2017				✓			
Shen et al. [20]	2017				✓			
Wei et al. [21]	2018				✓			
Xu et al. [22]	2020				✓			
Jobson et al. [23]	1977					✓		
Jobson et al. [24]	1977					✓		
Guo et al. [25]	2016						✓	
Wang et al. [26]	2013					✓	✓	
Fu et al. [27]	2016					✓	✓	
Fu et al. [28]	2019					✓	✓	
Li et al. [29]	2018					✓	✓	✓
Ren et al. [30]	2018					✓	✓	✓

GT methods directly modify the gray values of low-light images using linear or nonlinear transformation functions [31]. The GT is an efficient method which can be easily applied to low-light images in order to increase the contrast and illumination [13][32]. In GT methods the calculations are carried out on each pixel individually without considering the relationship with its neighbors [25], therefore, the results may be vulnerable and visually inconsistent [13][25].

Inadequate ability to increase the contrast of low-light images, excessive brightness and loss of some visual details are the main drawbacks of GT methods [30][32].

HE is another method that has been widely used to enhance low-light images by equalizing the histogram of gray values [33][9]. Typically, HE normalizes the gray values in the range [0,1] to prevent the saturation of relatively bright areas and consequently preserving the image details [25]. HE methods can be categorized as follows [34][35]:

- Global Histogram Equalization (GHE)
- Local Histogram Equalization (LHE)

GHE (e.g. [14][16][15]) uses the entire gray levels histogram information of an input image. GHE based methods mainly try to recreate the gray levels of the image based on the cumulative density function [36]. This approach is suitable for overall image enhancement, but fails in small gray levels [34][16]. To solve this problem, LHE approach (e.g. [17][18][19]) is recommend where for each pixel, a small window is created containing the neighboring pixels. Then the gray value of pixel is determined based on information obtained from its neighbors[16]. So, LHE is less sensitive to high-frequency levels [19] but suffers from high computational cost, noise sensitivity, and unnatural color rendering [34][36].

Recently data-driven based techniques such as machine learning techniques have also been used to enhance low-light images (e,g. [8][20][21][22][40]). Yang et al. [40] presented a low light image enhancement method using coupled dictionary learning. Lore et al. [8] explored two types of deep architecture ((LLNet and SLLNet) for simultaneous and sequential learning of contrast-enhancement and denoising. Shen et al. [20] showed that MSR is equivalent to a feed-forward convolutional neural network with different Gaussian convolution kernels. Accordingly, they presented a deep convolutional neural network (MSR-net) to enhance low-light images. Generally, Machine learning based methods could provide acceptable enhancement but demand high computation and reliable training datasets [9]. Because real data paired with normal light and low-light is difficult to collect, these methods may not fully characterize the formation of natural images in low light and lead to unnatural results [30].

Retinex theory is another method that has been welcomed by researchers to enhance low-light images. Retinex theory decomposes an image into two factors: reflectance and illumination [20].The illumination factor determines the amount of light intensity on objects and the reflection factor determines the physical properties of objects [27]. In some studies, both reflectance and illumination are estimates (e.g. [27][37][38][26][28]), but in some other studies, in order to reduce the computation, only one of these factors is estimated and the other factor is calculated based on the estimated factor (e.g. [25][24][23]). Early attempts such as single-scale Retinex (SSR) [23] and Multi-Scale Retinex (MSR) [24] considered the reflection factor as the final enhanced result and then calculated the illumination factor using the reflection natural logarithm [29]. Excessive illumination and unnatural appearance of image colors are the disadvantages of these two research [25]. Multi-scale Retinex method with color restoration (MSRCR) [24] can eliminate these shortcomings. Although this method eliminates the problem of color distortion to some extent, it may not be able to preserve the image detail well, especially in bright areas [39]. In order to increase the quality of enhanced images, Wang et al. [26] proposed a mathematical model for simultaneous reflectance and illumination estimation (SRIE). Although SRIE results in impressive images [29], it mostly does not uniformly distribute the illumination and in some cases generates halo artifacts [30]. Also, simultaneous estimating reflection and illumination lead to a significant increase in computational cost [25]. To deal with this, the method of *Low-light Image Enhancement via Illumination Map Estimation (LIME)* [25] acquires only the illumination factor using a mathematical model. Authors of LIME claimed that their method worked better than SRIE which estimated both reflection and illumination. Although the visual quality of enhanced images by LIME is often desirable, but since the reflection is not estimated, some detail in the bright area may be lost and also may observe more noise in enhanced images [29][30]. To deal with this Ren et al. [30] estimated simultaneously reflection, illumination and noise by developing the mathematical model of SRIE. Li et al. [29] argued that simultaneous estimation of reflection and illumination could make more noise, so they estimated illumination and reflection in two Sequential mathematical models, respectively.

So far, different mathematical models such as [25][26][29][30] based on Retinex theory have been proposed. Most of these models (such as [26][29][30]) estimate both reflectance and illumination in order to achieve impressive images. Increasing computational time is a major challenge in these methods. For this reason, some other models, such as LIME, only estimate the illumination factor. But, if the illumination is not estimated correctly, it can cause losing details and excessive illumination in enhanced images. For this reason, this article tries to estimate the illumination map more accurately than the mentioned models.

The objective function of the mathematical models mentioned above is not differentiable. For this reason, classic optimization methods such as Newton, Gradient and Trust Region cannot be used to obtain the global optimal solution. This paper presents a differentiable mathematical model and convex with linear constraints that can provide a chance to acquire global optimum solution. It is expected that the estimated illumination by proposed model will result in more impressive images compared to other models. Because achieving the global optimal solution takes a lot of computational time, this article also presents a heuristic approach to fast solve the proposed mathematical model with acceptable accuracy.

The remainder of this paper is organized as follows. Section 2 explains the proposed method in detail. Section 3 introduces several scales for assessing the visual quality of enhanced images. In Section 4, the propose methods are evaluated equally and in section 5, the achieved results are presented and discussed.

2. Proposed Method (*IMS*)

As it was reviewed in the previous section, direct increase in the brightness of low-light images (GT based methods) can lead to loss of details particularly in bright spots [32]. HE methods mostly cannot increase the brightness of low-light images well [25]. Machine learning based methods could provide acceptable enhancement but demand high computation and reliable training datasets [9]. Among the techniques which were summarized in Table 1, those methods which built based on Retinex theory could provide a chance to simultaneously improve the illumination and contrast of low-light images [17]. so far, different mathematical models (such as LIME [25], JED [30], JIEP [41], SRRLI [29] and SRIE [27]) based on this theory have been proposed. The objective function of the mentioned mathematical models is not differentiability, this can make it difficult to achieve the global optimal solution. This paper presents a differentiability mathematical model and convex with linear constraints that can provide a chance to acquire the global optimum solution. The proposed method uses this model to smooth the illumination map, for this reason, we call this method Illumination Map Smoothing (*IMS*). *IMS* enhances low-light images using Retinex theory. It is expected that *IMS* could improve the readability of low-light images within a practically short elapsed time. Moreover, *IMS* is supposed to be hired for real-time computer vision applications on poor processors such as mobile devices.

Retinex theory decomposed images into two factors; reflection and illumination Eq. (1):

$$L = R \circ T \tag{1}$$

where L represents the initial low-light image and R and T represent the enhanced image and the illumination map, respectively. Also in Eq. (1) the operator $\circ$ means element-wise multiplication. Accordingly, in order to increase the brightness of an image in low light, the *IMS* estimates a suitable illumination map (T) for each image. For this purpose *IMS* first, obtains the initial illumination map ($\hat{T}$) of the image from Eq. (2).

$$\hat{T}(x,y) = \max_{c \epsilon \{R,G,B\}} L^c(x,y) + \epsilon \tag{2}$$

where ϵ is a very small constant and it is used to prevent the denominator of Eq. (3) from becoming zero. Also, R, G and B indicate the color value of Red, Green and Blue channels, respectively. By replacing $\hat{T}$ in Eq. (3), raw bright image ($\hat{R}$) is obtained.

$$\hat{R} = L/\hat{T} \tag{3}$$

As shown in Fig. (1), $\hat{R}$ is often much brighter than L. The histograms related to these two images also show this fact.

Initial low-light image (L)	**Raw bright image ($\hat{R}$)**	**Recovered image ($\bar{R}$)**	**Enhanced image (R)**

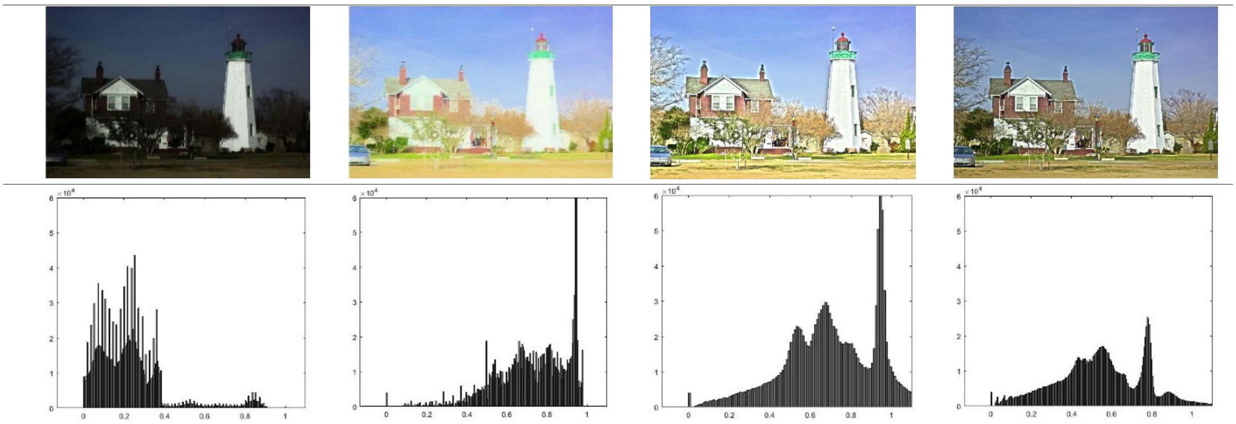

Fig 1: Comparison of initial low-light image (L), raw bright image ($\hat{R}$), recovered image ($\bar{R}$) and enhanced image (R) with their histograms.

As in Fig. (1) can be seen, many of the image important details are lost in $\hat{R}$. *IMS* in order to recover lost details by solving a novel mathematical model does more smoothness initial illumination map ($\hat{T}$). Smoothing the illumination map using the global optimal solution is called *Illumination Map Optimal Estimation (IMOE). IMOE* requires a lot of computational time to smooth the illumination map. In this paper, a heuristic method is proposed to faster solve the mathematical model. Smoothing the illumination map using this initiative is called *Illumination Map Heuristic Estimation (IMHE). IMOE* and *IMHE* approaches are explained in detail in Section 2.1. The illumination map estimated from these two approaches is called recovered illumination map ($\bar{T}$) and also we call $\bar{R} = \frac{L}{\bar{T}}$ recovered image ($\bar{R}$).

As shown in Fig. (1), histogram of recovered image ($\bar{R}$) is more smoothed than raw bright image ($\hat{R}$). For this reason, $\bar{R}$ has a better visual quality compared to $\hat{R}$. However, due to the high brightness, the colors in $\bar{R}$ still look somewhat unnatural. Also, some details are not visible in $\bar{R}$. To address these shortcomings, *IMS* uses a simple Linear Transformation (LT) to correct recovered illumination map ($\bar{T}$). *LT* uses Eq. (4) to correct images:

$$T = \bar{T} + \omega \tag{4}$$

where ω is a parameter for adjusting the illumination. If ω is selected less than zero, the brightness of the image will increase, and if it is selected greater than zero, the brightness of the image will decrease. Since the brightness of recovered images is mostly high, ω should be greater than zero to reduce the brightness. The corrected illumination map is called enhanced illumination map (T) and also we call $R = \frac{L}{T}$ enhanced image (R). As can be seen in Fig. (1), enhanced image (R) has desirable illumination and visual quality. The *IMS* steps can be seen in Fig. (2).

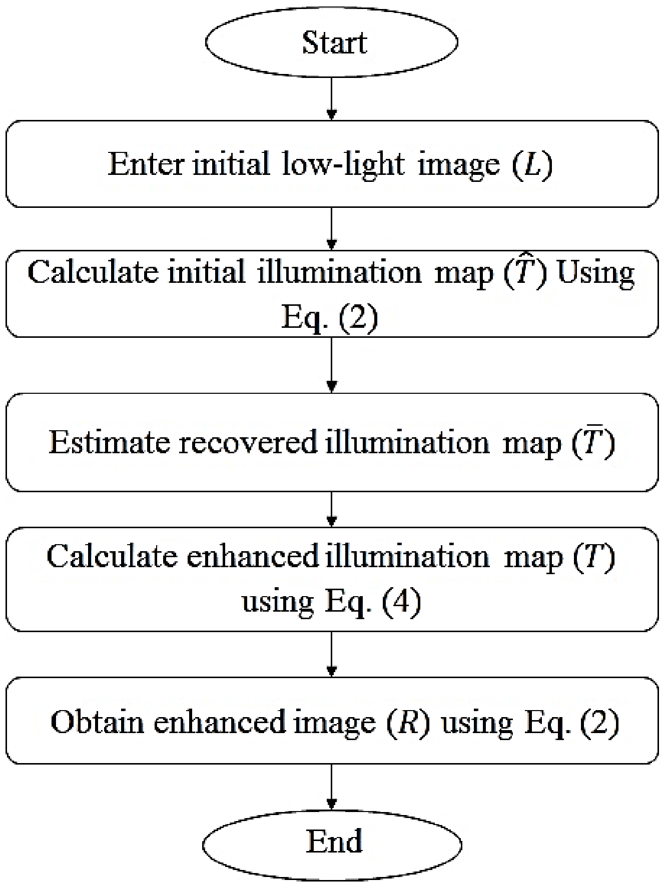

Fig 2: *IMS* algorithm

2.1 Illumination map estimation approaches

In this section, two different estimation methods (*IMOE* and *IMHE*) for determining recovered illumination map ($\bar{T}$) are presented. *IMOE* method seeks for best $\bar{T}$ by searching the entire solution space which demands a huge computation time. *IMHE* method aims to have a near optimum solution but in real-time. In both methods the following assumptions are being taken into account:

- Recovered illumination map ($\bar{T}$) does not differ much from initial illumination map ($\hat{T}$) (To maintain image illumination).
- In recovered illumination map ($\bar{T}$), the value for each pixel should be as close as possible to the neighbor pixels (To enhance image quality and smoothness).

In a recovered illumination map ($\bar{T}$), although minimizing the difference between illumination values of neighbor pixels could improve the visual quality, a big difference between illumination value of each pixel and its corresponding value in $\hat{T}$ might make the image so dark. Thus in the two proposed approaches it is tried to balance between the two above-mentioned issues in order to enhance illumination while keeping the image readability. Generally, it can be said that the proposed approaches seek to smooth initial illumination map ($\hat{T}$).

2.1 Illumination Map Optimal Estimation (*IMOE*)

In the literature, a wide range of techniques for light enhancement have been introduced (such as LIME [25], JED [30], JIEP [41], SRRLI [29] and SRIE [27]) which their objective function are not differentiable. For this reason, many optimization methods classic such as Newton, gradient and Trust Region methods cannot be used to achieve the global optimal solution of these models [42]. In this paper an attempt is made to propose a differentiable and convex model in order to achieve the global optimal solution value of $\bar{T}$. The proposed model is as follows:

$$\min_{T} \sum_{i=1}^{m} \sum_{j=1}^{n} \left(\bar{T}(i,j) - \hat{T}(i,j)\right)^2 \tag{5}$$

$s.t$

$$\bar{T}(i,j) = \frac{\alpha\hat{T}(i,j)+W_{ij}(i-1,j)\bar{T}(i-1,j)+W_{ij}(i+1,j)\bar{T}(i+1,j)+W_{ij}(i,j-1)\bar{T}(i,j-1)+W_{ij}(i,j+1)\bar{T}(i,j+1)}{\alpha+W_{ij}(i-1,j)+W_{ij}(i+1,j)+W_{ij}(i,j-1)+W_{ij}(i,j+1)} \tag{6}$$

Eq. (5) ensures that $\bar{T}$ does not differ much from $\hat{T}$. Hence it can be ensured that $\bar{R}$ has the necessary illumination. In order to improve smoothness of the initial illumination map ($\hat{T}$), Eq. (6) is added to model as main constraint to maintain the illumination value of each pixel as close as possible to the neighbor pixels. α is a calibration parameter larger than zero. If a close value to zero is assigned to α, a smoother $\bar{T}$ is obtained. If a large value is assigned to α, $\bar{T}$ will be numerically closer to $\hat{T}$ which lead to a very bright image.

In Eq. (6), W is weight matrix, which determines the effect of the neighbors of a pixel. In the literature two main strategies have been introduced to calculate the weight matrix (W) [25]:

I. **Weightless strategy**: In this strategy, the effects of all neighboring pixels are considered the same. So, weights of all pixels are considered equal to 1.

II. **Weighted strategy:** In this strategy, for each pixel, the effect of neighboring pixels with values of similar brightness to the central pixel is more considered.

$$W_{ij}(m,n) = \frac{1}{\left|\hat{T}(i,j) - \hat{T}(m,n)\right| + \epsilon} \tag{7}$$

where $W_{ij}(m,n)$ specifies the effect of the pixel (m,n) on the pixel (i,j).

Acquiring global optimum solution of $\bar{T}$ for large instances might be computationally hard, so in the following section a heuristic method is proposed to find a near optimum solution for $\bar{T}$ with less time cost.

2.1.1 Illumination Map Heuristic Estimation (*IMHE*)

Given that the proposed mathematical model is a differentiable, convex model with linear constraints, it is possible to find the global optimal solution by using different optimization methods. But, since the exact solution of this model requires a high computational time (due to the high number of constraints because Eq. (6) is repeated for each pixel), *Algorithm 1* is developed to quickly find a near optimum solution for $\bar{T}$.

Algorithm 1 considers constraints of the proposed mathematical model (Eq. 6) as follows:

$$\bar{T}(i,j)-\hat{T}(i,j)=\frac{1}{\alpha}(W_{ij}(i-1,j)\bar{T}(i-1,j)+W_{ij}(i+1,j)\bar{T}(i+1,j)+W_{ij}(i,j-1)\bar{T}(i,j-1)+W_{ij}(i,j+1)\bar{T}(i,j+1) - (W_{ij}(i-1,j)+W_{ij}(i+1,j)+W_{ij}(i,j-1)+W_{ij}(i,j+1))\bar{T}(i,j)) \quad (8)$$

First, Eq. (8) ensures that any solution obtained by the heuristic approach does not violate the feasible region of the proposed model (Eq. 6). Second, left phrase of Eq. (8) is equal to the square root of objective function in proposed model (Eq. 5). So, global optimal solution of proposed model can be found among the solutions of Eq. (8). Suppose $\bar{T}_1, \bar{T}_2, \dots, \bar{T}_n$ are solutions for Eq. (8). $\bar{T}_p$ is global optimal solution of proposed model if and only if for each $1 \le q \le n$:

$$\sum_{i=1}^{m}\sum_{j=1}^{n}\left(\bar{T}_p(i,j)-\hat{T}(i,j)\right)^2 \le \sum_{i=1}^{m}\sum_{j=1}^{n}\left(\bar{T}_q(i,j)-\hat{T}(i,j)\right)^2 \quad (9)$$

For $\bar{T}=\hat{T}$, objective function (Eq. (6)) is equal to zero. For this reason, *Algorithm 1* uses $\hat{T}$ as initial solution ($\bar{T}^0=\hat{T}$). For $\bar{T}^0=\hat{T}$, left phrase of Eq. (8) is equal to zero but often in this case right phrase of Eq. (8) is much greater than left phrase of Eq. (8). Therefore, $\bar{T}^0$ should be changed so that right phrase of Eq. (8) decreases. In Eq. (8), the least value of right phrase occurs for $\bar{T}(i,j)$s that satisfy the following equation:

$$\bar{T}(i,j)=\frac{W_{ij}(i-1,j)\bar{T}(i-1,j)+W_{ij}(i+1,j)\bar{T}(i+1,j)+W_{ij}(i,j-1)\bar{T}(i,j-1)+W_{ij}(i,j+1)\bar{T}(i,j+1)}{W_{ij}(i-1,j)+W_{ij}(i+1,j)+W_{ij}(i,j-1)+W_{ij}(i,j+1)} \quad (10)$$

According to this, *Algorithm 1* applies changes on $\bar{T}^0$ to reduce right phrase of Eq. (8). For this reason, *Algorithm 1* calculates $\bar{T}^t$ in each iteration as follows:

$$\bar{T}^{t+1}(i,j)=\frac{W_{ij}(i-1,j)\bar{T}^t(i-1,j)+W_{ij}(i+1,j)\bar{T}^t(i+1,j)+W_{ij}(i,j-1)\bar{T}^t(i,j-1)+W_{ij}(i,j+1)\bar{T}^t(i,j+1)}{W_{ij}(i-1,j)+W_{ij}(i+1,j)+W_{ij}(i,j-1)+W_{ij}(i,j+1)} \quad (11)$$

Algorithm 1 should continue until $\bar{T}^t$ satisfies Eq. (8). In this case, $\bar{T}^t$ will be in feasible region of proposed mathematic model. Also, because $\hat{T}$ is used as the initial solution, we expect $\bar{T}^t$

not to differ much from global optimal solution (For $\bar{T}^0 = \hat{T}$ the value of the objective function is zero). The proposed algorithm is as follows:

Algorithm 1: A heuristic method for solving the mathematical model

Input: initial illumination map ($\hat{T}$)
1: Calculate the weight matrix W.
2: Set $\bar{T}^0 = \hat{T}$ and $t = 1$.
3: Do the following until the stop condition is met:
  a) Calculate $\bar{T}^t$ using Eq. (11).
  b) Set $t = t + 1$.
4: Set $\bar{T} = \bar{T}^t$.

Computational Complexity of *Algorithm* 1: The computational complexity of *Algorithm 1* for an image with N pixels is mainly determined by step 3 where for each pixel Eq. (11) must be calculated. The number of calculations performed in Eq. (11) for each pixel is of order $O(1)$. Due to fact that the input image has N pixels, $O(N)$ operations are performed in each iteration. Thus the computational complexity of *Algorithm 1* is equal to $O(tN)$ where t is equal to the number of *Algorithm 1* iterations.

3. Visual Quality Evaluation

This paper uses the following metrics to evaluate the visual quality of enhanced images:

- Absolute Mean Brightness Error (AMBE) [15]
- Lightness Order Error (LOE) [43]
- Blind/Reference less Image Spatial Quality Evaluator (BRISQUE) [44]
- Natural Image Quality Evaluator (NIQE) [45]
- Structural SIMilarity (SSIM)[46]
- Peak Signal-to-Noise Ratio (PSNR) [47].

AMBE measures the brightness of images so that for brighter images, AMBE is larger. LOE metric is used to measure the discrepancy in lightness order between an initial low-light image (L) and enhanced image (R). A smaller LOE means that the order of the image lightness is better preserved during processing. BRISQUE metric can be used to assess blurring and noise in an image. A smaller score indicates better perceptual quality. NIQE evaluates how natural an image looks, for more natural images this value is less. SSIM is used to evaluate the structural similarity between two images, and generally a larger SSIM means better processing. PSNR determines the degree of deviation from the original image based on human perception of contrast [8]. Higher PSNR indicates better image reconstruction. Generally, these metrics can be used to compare the visual quality of enhanced images.

4. Experiments and results

This paper presents a method which called Illumination Map Smoothing (*IMS*) to enhance illumination of low-light images. Using the proposed mathematical model (*IMOE*), *IMS* seeks for global optimum solution. *IMOE* is implemented in IBM ILOG CPLEX 12.10 on a machine with 8 GB of RAM and CPU core i5. Also, the heuristic approach (*IMHE*) is implemented in MATLAB R2017b package.

In section 4.1, the parameters of *IMS* are checked. Then in section 4.2, the performance of *IMS* is compared with popular methods such as DONG [48], NPE [26], SRIE [27], SRLLI [29], JED [30] and LIME [25]. In this evaluation, the images of references [25] and [30] are used. The AMBE [15], LOE [43], (BRISQUE) [44], NIQE [45], SSIM [46]and PSNR [47] metrics are used to make a qualitative comparison.

4.1 *IMS* parametric check

The *IMS* in order to estimates the recovered illumination map ($\bar{T}$) uses *IMOE* or *IMHE* approach. It then uses LT to improve image visual quality. In section 4.1, the performance of LT is examined. Then in section 4.2 parameters of *IMS* are investigated in two mode of *IMOE* and *IMHE*. Finally in section 4.3, the performance of *IMOE* and *IMHE* approaches are compared.

4.1.1 Parametric check of LT

Visual quality of recovered images ($\bar{R}$) obtained using *IMOE* and *IMHE* approaches are not desirable (as shown in Fig. 3). To tackle this issue, in the literature a couple of techniques were introduced (such as Gamma Correction and Linear Transformation) that could effectively enhance visual quality. In this paper to demonstrate how this process works, we implement LT. The most parameter in LT which must be determined is ω. If a big constant is assigned to ω, enhanced images become too dark, and if ω is a small number, the contrast of enhanced images would not improve quite well.

Generally, the correct value of ω should be selected by trial and error and according to the brightness of each image. According to Fig. (3) and other experiments performed by authors, commonly LT for ω = 0.08 works well in *IMS*. For this reason, in the continuation of this article, this value is used to correct images.

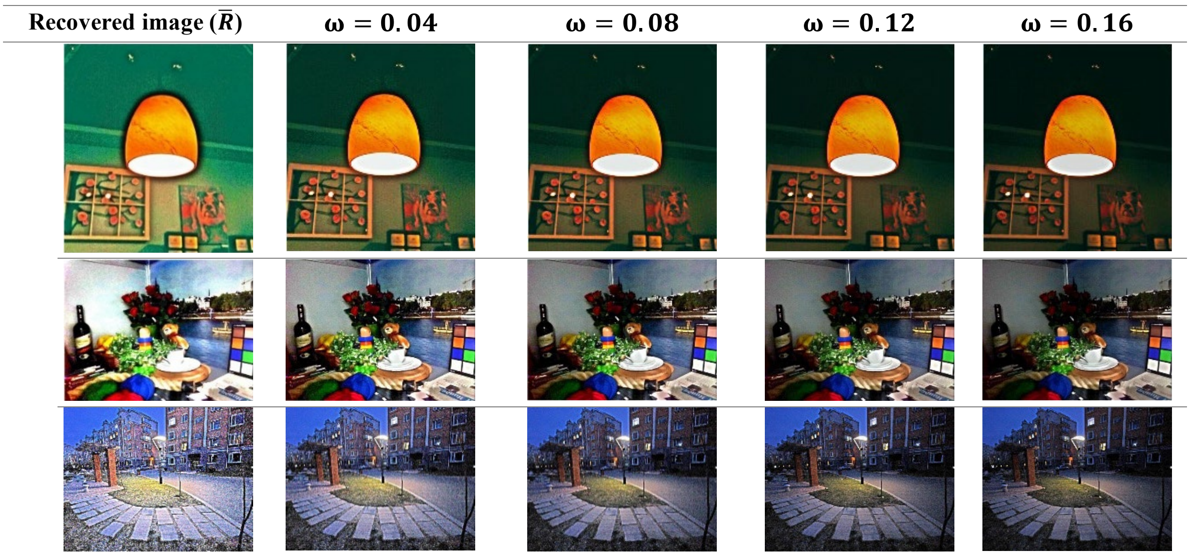

Fig 3: Parametric check of LT

Table 2 examines from the aspect of AMBE, LOE, BRISQUE, SSIM, PSNR and NIQE metrics the performance of LT by selecting $\omega = 0.08$. The numbers reported in this table are obtained by calculating the average of 10 images used in this article. From an AMBE metric perspective, LT reduces the illumination of $\bar{R}$ correctly. In addition, LT from the perspective of LOE, BRISQUE, SSIM, PSNR and NIQE metrics, increases the visual quality of $\bar{R}$. So, LT is effective in improving the visual quality of recovered images.

Table 2: Evaluation of LT efficiency using AMBE, LOE, BRISQUE, SSIM, PSNR and NIQE metrics

	AMBE	LOE	BRISQUE	SSIM	PSNR	NIQE
Recovered image ($\bar{R}$)	0.5927	2131	20.46	0.2317	5.79	3.70
Enhanced image (R)	**0.4092**	**969**	**17.09**	**0.3433**	**10.62**	**3.32**

4.1.2 Experiment of *IMOE* approach

When *IMS* uses the *IMOE* approach to estimate enhanced illumination map ($\bar{T}$), the following factors affect the visual quality of enhanced images (R):

I. Value of α parameter
II. Type of weight matrix calculation strategy (W).

Table 3 examines the effect of these parameters on the visual quality of enhanced images. If $\alpha = 0$ is selected, the visual quality of enhanced images is generally not desirable (e.g. images (b), image (e), image (i) and image (l) in Table 3). In this case, some details in enhanced images may be lost. If α is set to 0.5 then the readability of the images is improved (e.g. images (c), image (j), image (f) and image (m) in Table 3). Generally details in enhanced images rises with α is increased. Excessive increasing α may cause unnatural colors in the enhanced images (e.g. images (d), image (k)). According to experiments performed by the authors, generally for different images, selecting $\alpha = 0.5$ gives a desirable output. Finding the optimum value for α could be consider as future works.

Table 3: Investigation effect of α and W on the visual quality of images

Initial image	Weightless strategy			Weighted strategy		
	$\alpha = 0$	$\alpha = 0.5$	$\alpha = 1$	$\alpha = 0$	$\alpha = 0.5$	$\alpha = 1$
 (a)	 (b)	 (c)	 (d)	 (e)	 (f)	 (g)
 (h)	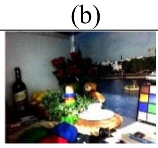 (i)	 (j)	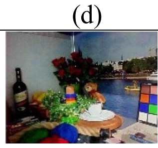 (k)	 (l)	 (m)	 (n)

In Table 3 you can also see the difference between using two strategies for calculating weight matrix (W). Generally in the *IMOE* approach, weighted strategy in comparison to weightless strategy have led to a higher quality (Table 3). So, in this paper, weighted strategy is selected to be used in *IMOE*.

4.1.3 Experiment of *IMHE* approach

When *IMS* uses the *IMHE* to estimate enhanced illumination map ($\bar{T}$), the following factors affect the visual quality of enhanced images (R):

I. Weight matrix calculation strategy (W)
II. Iterations number of *Algorithm 1*

To achieve an image with desired visual quality, the above factors should be adjusted according to brightness. In *IMHE*, unlike *IMOE*, weightless strategy is more cost-effective without compromising the visual quality. As it can be seen in Table 4, when the weightless strategy is used, the colors of the enhanced images look a bit more natural. This is also confirmed by *NIQE* metric.

Table 4: Investigating the difference between weightless strategy and weighted strategy in the *IMHE* approach

Weightless strategy				
Time	**0.32**	**0.21**	**0.72**	**0.30**
NIQE	**2.42**	**4.60**	**2.49**	**4.41**
weighted strategy				
Time	1.08	0.69	2.18	1.05
NIQE	2.48	4.87	2.59	4.53

Fig. (4) is depicted to investigate the quality of the enhanced images when iteration number of *Algorithm 1* is varied. As it can be seen in this Table, after 50 iterations the quality of enhanced images have not been changed significantly and after 1000 iterations the visual quality is started to be deteriorated (for example, in Fig. (4a) the area around the lamp is blacked, in Fig. (4b) the details of mug are lost, in Fig. (4c) pink flower color is changed to white, and in Fig. (4d) details of clouds are almost lost). So, *IMHE* is terminated after 50 iterations.

Therefore, iterations number of *Algorithm 1* should not be selected very much or very little. Often, by selecting 50 to 100 iterations the desired visual quality can be achieved. On the other hand, *Algorithm 1* is not a very cheap computational process, So it seems that choosing 50 iterations for *Algorithm 1* is better decision.

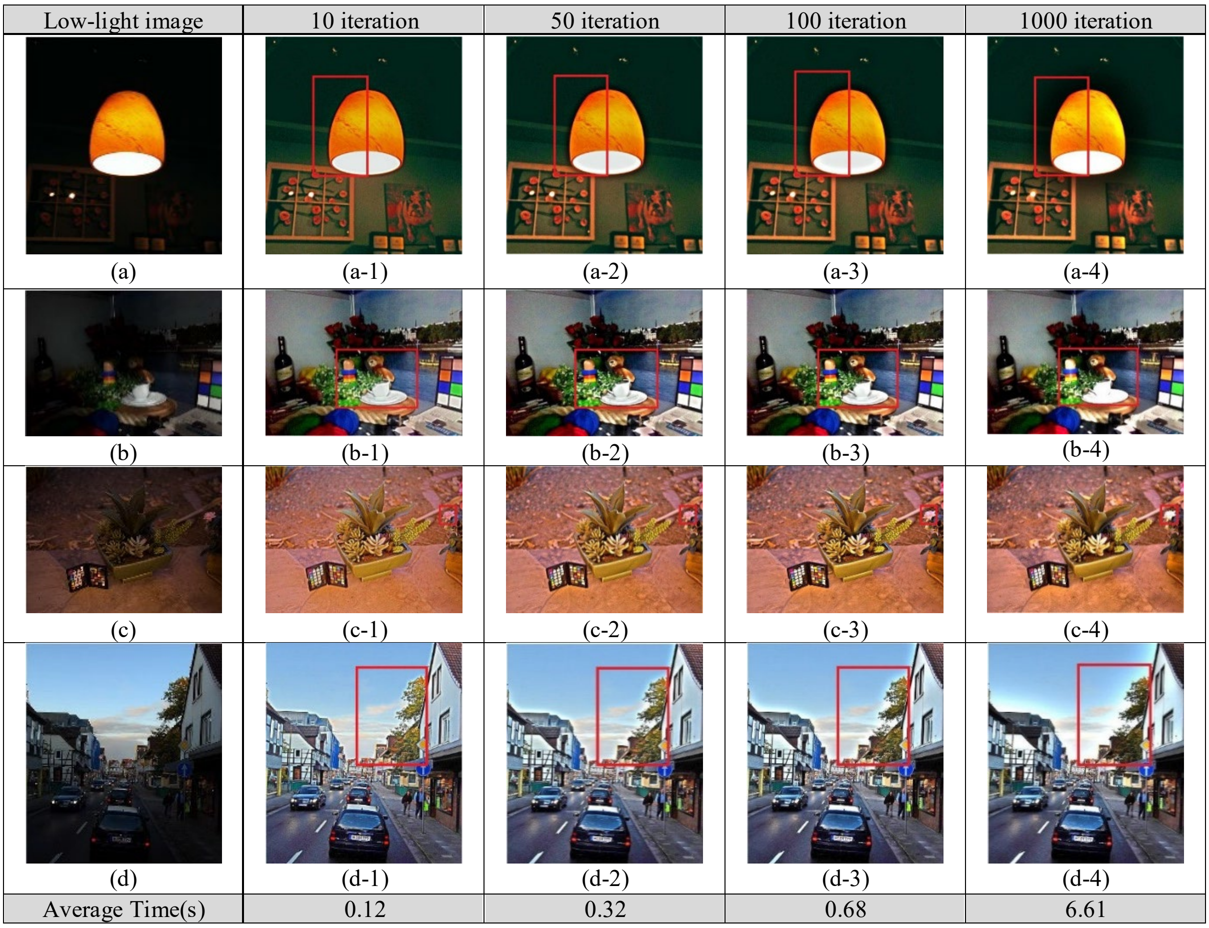

Fig 4: Check iterations number in *IMHE* approach

4.1.4 Comparison of *IMOE* and *IMHE* approaches

As it was described in details, this paper proposes two approaches (*IMOE* and *IMHE*) to estimate the recovered illumination map. *IMOE* seeks for optimum solution, while *IMHE* is a heuristic based method looking for a near optimum solution but within a very short computation time.

In this section, *IMOE* and *IMHE* are compared using AMBE, LOE, BEISQE, NIQE, SSIM and PSNR metrics and also computational time.

As it can be seen in Fig. (5) and Table 5, in terms of visual quality, there is not much difference between *IMOE* and *IMHE* approaches. But *IMOE* takes very more time to calculate the recovered illumination map ($\bar{T}$) in comparison with *IMHE* (Table 5). For this reason, in the following section to compare *IMS* with other similar methods, we use the IMHA approach to estimate the recovered illumination map.

Fig 5: Comparison of the performance of *IMOE* and *IMHE*

		AMBE	LOE	BRISQUE	NIQE	SSIM	PSNR	Time
Image (a)	*IMOE*	0.2122	**821**	**31.70**	**4.20**	**0.2396**	**15.41**	10.25
	IMHE	**0.2142**	878	31.82	4.41	0.2323	15.26	**0.32**
Image (b)	*IMOE*	0.3326	816	**8.16**	2.54	**0.3350**	**12.10**	35.10
	IMHE	**0.3341**	**778**	9.30	**2.49**	0.3312	12.01	**0.72**
Image (c)	*IMOE*	**0.3712**	656	**10.09**	2.45	**0.2707**	9.70	7.27
	IMHE	0.3687	**640**	15.50	**2.40**	0.2615	**9.78**	**0.28**
Image (d)	*IMOE*	0.5305	**1256**	**9.31**	4.89	**0.4971**	**10.39**	5.40
	IMHE	**0.5358**	1373	9.62	**4.60**	0.4854	9.92	**0.24**
Image (e)	*IMOE*	**0.4024**	976	16.75	2.48	**0.4159**	10.85	8.50
	IMHE	0.4019	**956**	**16.50**	**2.42**	0.4119	**10.86**	**0.32**

Table (5): Comparison of *IMOE* and *IMHE* approaches in terms of LOE, BEISQE, NIQE, SSIM and PSNR metrics and execution time.

4.2 Comparison of *IMS* with other similar methods

In this section, *IMS* performance is compared with competitor methods including DONG [47], NPE [23], SRIE [24], SRLLI [26], JED [27] and LIME [22]. The test images are borrowed from [22] and [27]. To quantify the visual quality 6 different metrics are used including AMBE [15], LOE [42], BRISQUE [43], NIQE [45], SSIM [44] and PSNR [46].

Fig. (6) compared the performance of IMS with other competitor methods on the test images.

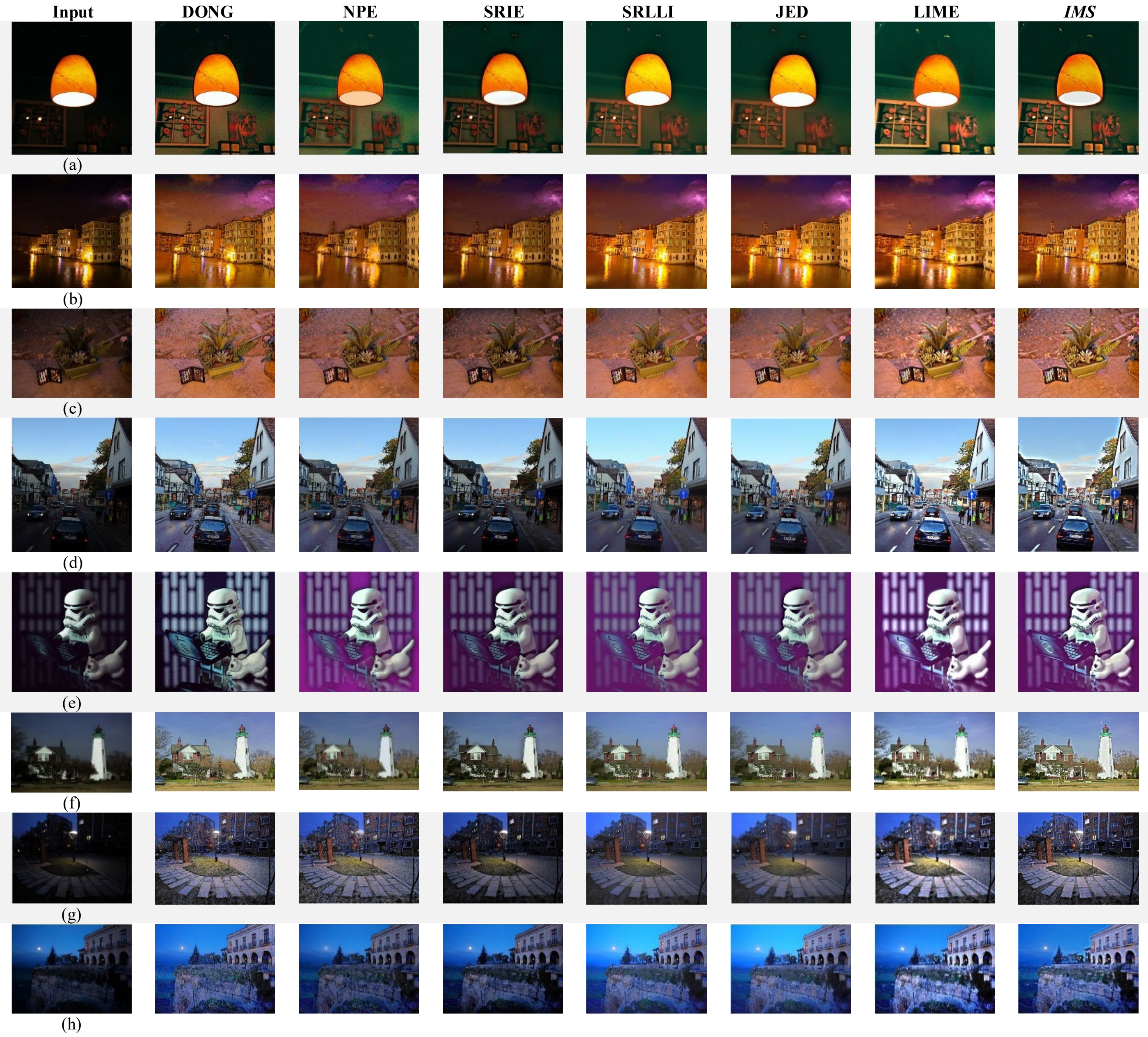

Fig 6: Enhancing low-light images using DONG [48], NPE [26], SRIE [27], SRLLI [29], JED [30] LIME [25] and *IMS* methods.

According to Fig. (6), *IMS* provided promising results and visually outperformed DONG and NPE (especially for Figs (6a), (6b) and (6d)). Enhanced images by DONG and NPE are often unnatural, this shortcoming is not seen in the enhanced images by *IMS*. In addition, *IMS* have provided images with a higher brightness (e.g. Figs (6c), (6d) and (6h)). Although the visual quality of enhanced images by SRIE is better than DONG and NPE, the visual quality of enhanced images by *IMS* is better than SRIE. In terms of brightness, SRIE has a weaker performance compared to the other similar methods which have led to lose details in the enhanced images by SRIE (e.g. Figs (6a) and (6d)) while it is not the case in the enhanced images by *IMS*.

The visual quality of enhanced images by JED and SRLLI are very similar to each other which in some cases (e.g Figs (6a), (6d) and (6g)) led to blurriness and losing some important details.

This shortcoming can impair the performance of computer vision algorithms such as object detection. Enhanced images by LIME are mostly clear, bright and desirable. As shown in Fig. (6), LIME and *IMS* supplied almost similar outcomes, so six image quality assessment metrics (AMBE, LOE, BRISQUE, NIQE, SSIM and PSNR) are used to quantify the visual characteristic of the enhanced images.

AMBE (↑) metric is used to evaluate the brightness of images. Fig. (7) shows the AMBE metric for the test images enhanced by *IMS* and other similar methods. According to the results, SRIE achieved lowest AMBE values and LIME and *IMS* respectively achieved the best performance.

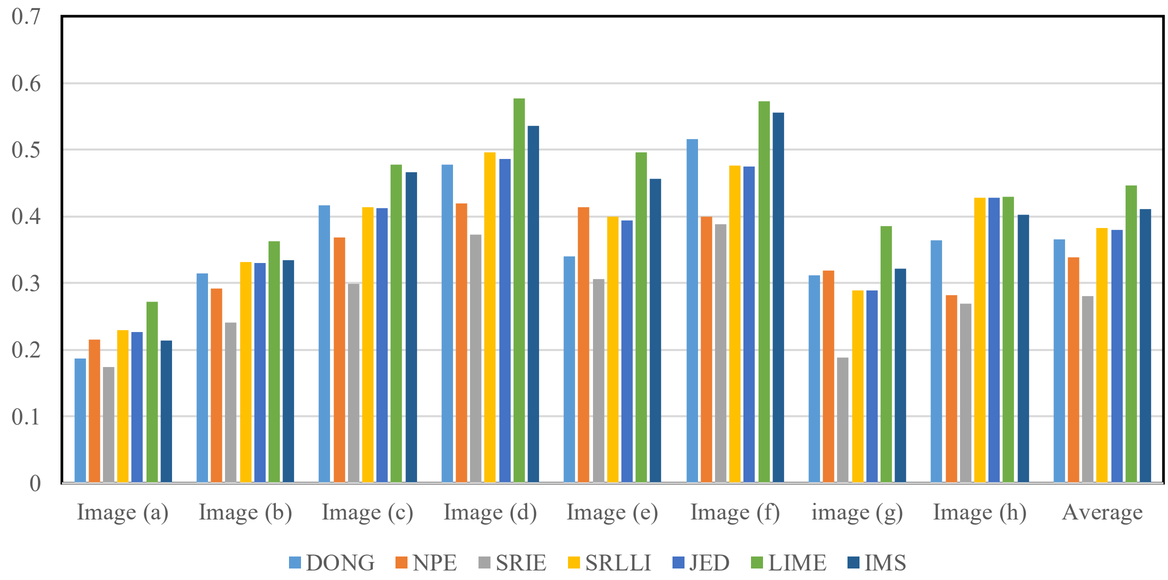

Fig 7: Evaluation of the test images using AMBE (↑) metric

AMBE metric only measures the brightness, but LOE, BEISQE, NIQE, SSIM and PSNR metrics could take into account other factors such as blurring, contrast, distortion and noise.

The LOE (↓) metric is used to measure the discrepancy in lightness order between an initial low-light image and its enhanced image. A smaller LOE means that the order of the image lightness is better preserved during processing. In Fig. (8), the test images are compared in terms of the LOE where *IMS* performed better than DONG and NPE, SRIE, JED and LIME in 5, 4, 3, 5 and 6 cases, respectively. As shown in Fig. (8), the *IMS* method performed much better than the SRLLI in all cases. In average, *IMS* compared to DONG, NPE, SRILI, JED and LIME achieved better LOE while SRIE performed a bit better than *IMS*.

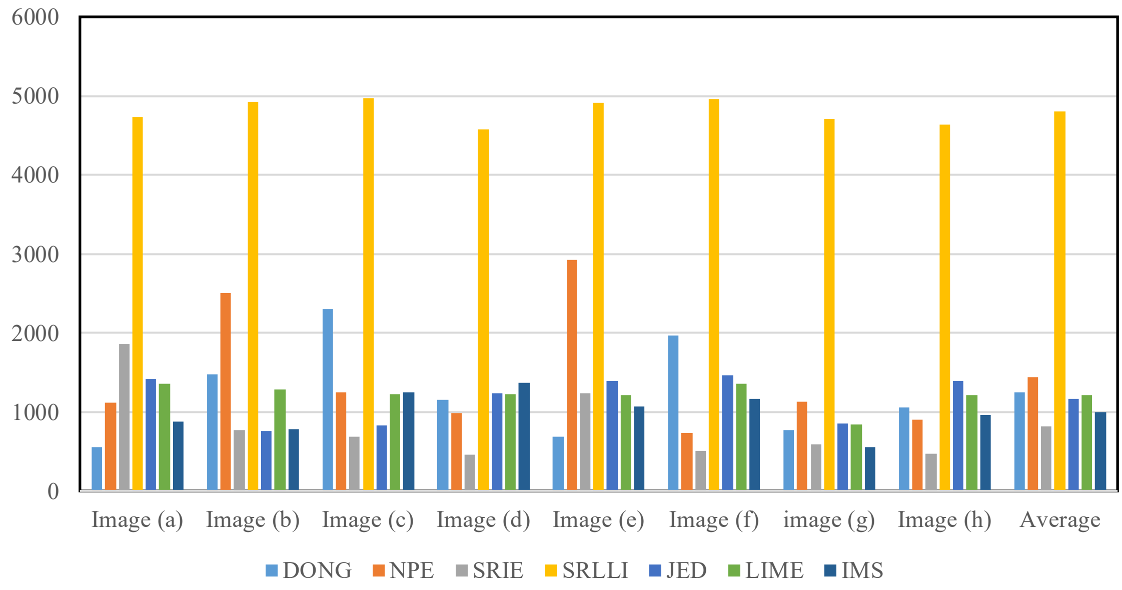

Fig 8: Evaluation of the test images using LOE (↓) metric

BRISQUE (↓) metric can be used to assess blurring and noise in an image. In Fig. (9) using BRISQUE metric, the test images are evaluated. The achived results show that *IMS* has performed better than DONG, NPE, SRIE, SRLLI, JED and LIME in images (f), (d),(e),(e), (g), (g) and (d) 4 respectively. In average, in terms of BRISQUE metric, enhanced images by *IMS* method are better than all other competitor methods (especially DONG, SRLLI and JED).

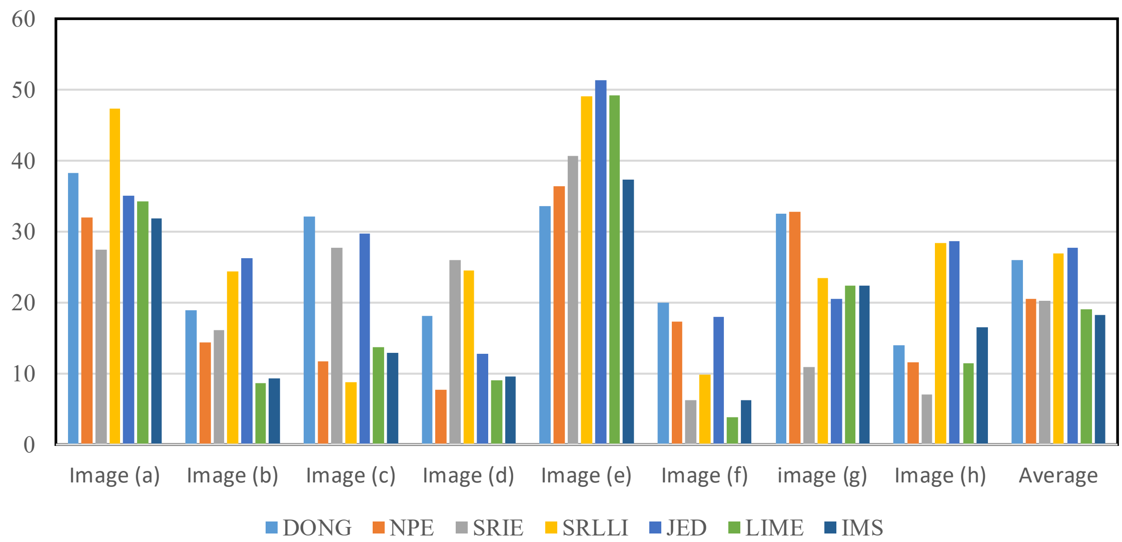

Fig 9: Evaluation of the test images using BRISQUE (↓) metric

NIQE (↓) metric evaluates how natural an image is. In Fig. (8), the test images are compared in terms of the NIQE where *IMS* performed better than DONG, NPE, SRIE, SRLLI, JED and LIME in images (f), (d), (b), (f), (d) and (g), respectively. In average, *IMS* compared to DONG, SRLLI and LIME achieved better NIQE.

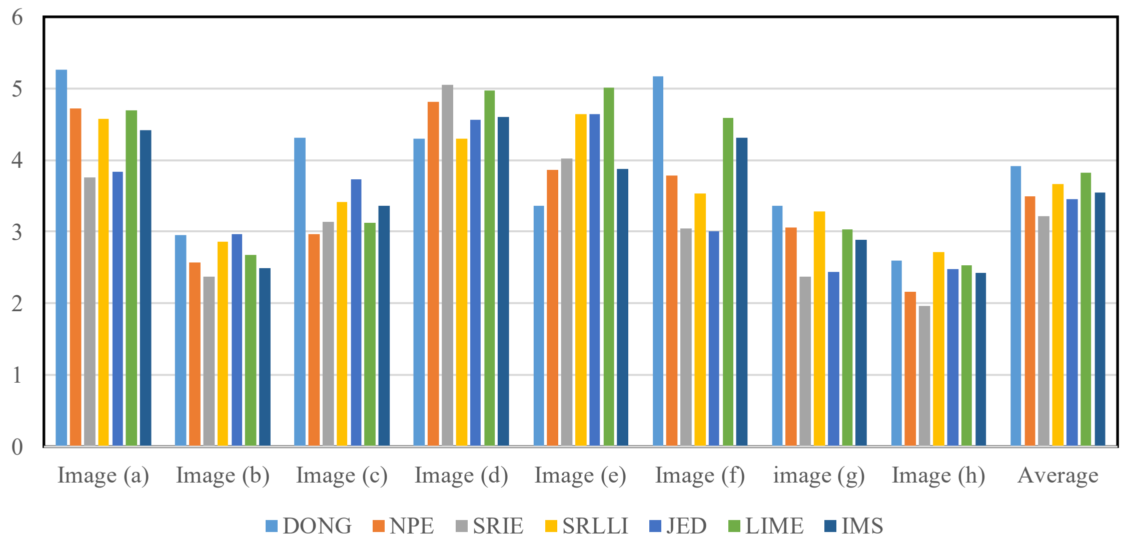

Fig 10: Evaluation of the test images using NIQE (↓) metric

SSIM (↑) metric is used to evaluate the structural similarity between the initial low-light image and the enhanced image. Also, PSNR (↑) metric determines the amount of deviation from the initial low-light image based on human perception of contrast [8]. SSIM and PSNR metrics for test images are reported in Figures 11 and 12, respectively.

In terms of SSIM and PSNR metrics, *IMS* is better than other methods whenever it undergoes fewer changes to images during processing. But it should be noted that to increase the brightness of a low-light image, changes must be made accordingly. So a higher of these two metrics do not necessarily mean a better enhancement of an image. In other words, in analyzing an image using these two metrics, its brightness (AMBE metric) should also be considered simultaneusly. For example, according to Figures 11 and 12, DONG, NPE and SRIE compared to *IMS*, LIME, JED and SRLLI have made fewer changes to the original images. But as shown in Fig. (6) and Fig. (7) enhanced images by SRIE, NPE and DONG are less bright than enhanced images by *IMS*, LIME, JED and SRLLI methods. This happened because the changes made by SRIE, NPE and DONG were not enough, SSIM and PSNR for these methods are not included in the advantage. Therefore for these two metrics, we only compare *IMS* with LIME, JED and SRLLI.

In terms of SSIM metric, *IMS* performed better for all the test images compared to SRLLI, JED and LIME. Also, in terms of PSNR metric for all the test images, *IMS* performance compared to SRLLI and LIME is significantly better. *IMS* compared to JED achieved better LOE in 3 cases. Based on these results, it is expected that more details can be seen in enhanced images by *IMS* compared to SSRLI, JED and LIME.

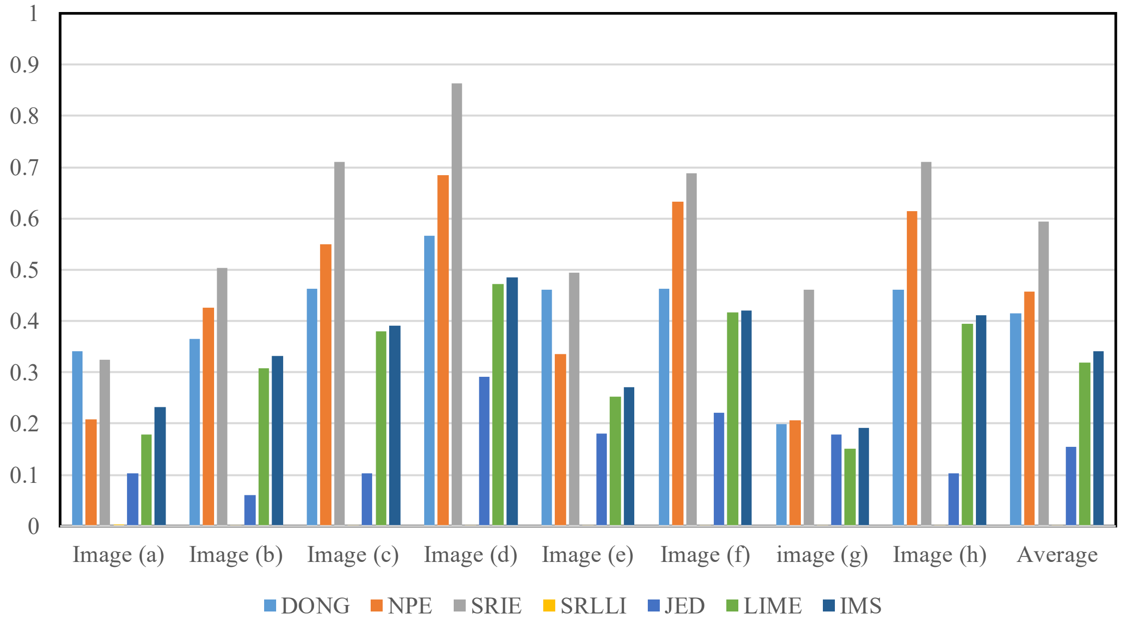

Fig 11: Evaluation of test images using SSIM (↑) metric

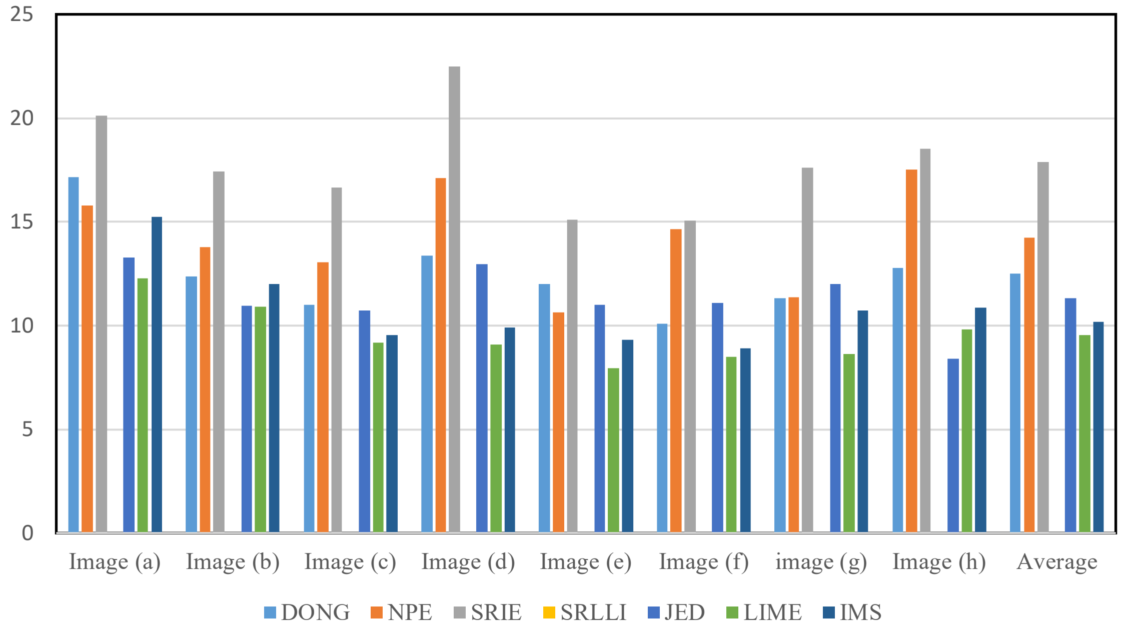

Fig 12: Evaluation of test images using PSNR (↑) metric

In Table 7, the computational time of DONG, NPE, SRIE, SRLLI, JED, LIME and *IMS* methods for test images is reported. As can be seen, the computational time of *IMS* is less compared to all other methods (especially SRLLI, SRIE, NPE and JED).

Table 7: Computation time of DONG, NPE, SRIE, SRLLI, JED, LIME and *IMS* methods for test images

	(a)	(b)	(c)	(d)	(e)	(f)	(g)	(h)	(i)
DONG	0.37	0.79	0.38	0.31	**0.32***	0.86	1.45	0.45	0.35
NPE	9.91	20.80	8.51	6.81	9.22	20.1	34.13	11.70	7.82
SRIE	17.62	25.92	8.92	17.63	10.21	34.2	170	17.79	20.01
SRLLI	34.31	63.23	12.32	14.12	12.41	43.2	97.31	16.48	17.31
JED	3.60	8.48	2.82	2.50	2.85	7.8	17.70	3.77	2.97
LIME	0.76	1.50	0.75	0.63	0.84	1.54	2.54	0.91	0.73
IMS	**0.32**	**0.72**	**0.31**	**0.24**	**0.32**	**0.67**	**1.25**	**0.32**	**0.28**

In summary and according to the above-mentioned results, the proven advantages of *IMS* compared to other similar methods are obvious. *IMS* in term of AMBE, LOE, BRISQUE, NIQE, SSIM and PSNR was ranked 2, 2, 1, 4, 4 and 5, respectively, and was faster in terms of implementation time than all other methods.

5. Discussion

This paper presents a new mathematical model called Illumination Map Smoothing (*IMS*) to robustly enhance low light images. In the proposed mathematical model, the smoothing of the illumination map is included in the model constraints and is done separately for each pixel. In similar mathematical models, the smoothing of the illumination map, along with other factors, is in the objective function. Smoothing in such cases can be influenced by other factors of the objective function (especially if the balance between the factors of the objective function is not well set). Providing a multi-objective mathematical model instead of placing contradictory factors in an objective function can be considered as future tasks. In the objective function of the proposed mathematical model, compared to similar models, only proximity to the initial illumination map is optimized. For this reason, according to AMBE metrics, IMS often results in more bright images compared to DONG, NPE, SRIE, SRLLI and JED.

In terms of BRISQUE and LOE metrics, IMS was ranked first and second, respectively. This could be due to better smoothing of the illumination map in proposed mathematical model (smoothing in constraints).

In terms of SSIM and PSNR, the proposed model makes fewer changes than SRLLI, JED and LIME in the original images. This is because the constraints of the proposed model (Eq. 6 or Eq. 8) limit the difference from the initial illumination map for each pixel. This limitation is not seen in other similar models.

IMS had less computational time compared to other methods. This is because in IMS method, unlike SRIE, SRLLI, JED and LIME only the illumination factor is estimated. Of course, LIME method also only estimated the illumination factor, but its computational complexity ($O(tNlogN)$) is more lorge than IMS ($O(tN)$). Given that for IMS 50 iterations are sufficient, its computational complexity ($O(50N)$).) becomes a desirable value.

In summary, IMS performs considerbaly better than other similar methods because *IMS* is the only differentiabile and convex method provides a chance to obtain the global optimal solution.

Conclusion

This paper proposed a method called *Illumination Map Smoothing (IMS)* to enhance low-light images. The main idea of *IMS* is to smooth initial illumination map ($\hat{T}$). For this purpose, *IMS* first obtains initial illumination map ($\hat{T}$). Then estimates recovered illumination map ($\bar{T}$) by solving a new mathematical model (*IMOE*). The main advantage of the developed mathematical model compared to other similar models is convexity and differentiability of the objective function which provides a chance to acquire global optimum. The quadratic nature of objective function and linearity of constraints in the proposed model are other advantages of *IMS*. Rather than *IMOE* which provides global optimum solution but demands a considerable computations time, this paper also proposed a heuristic approach (*IMHE*) to quickly provide a near optimum solution for the mathematical model introduced. The results of section 4.1.4 shows that there is in terms of visual quality significant no difference between the exact solution supplied by *IMOE* and the *IMHE* output. However, the computational time of *IMHE* is much less compared to *IMOE*. So it seems more economical to use *IMHE* for estimating recovered illumination map ($\bar{T}$).

IMS uses a simple *Linear Transformation (LT)* to correct the illumination map ($\bar{T}$). In section 4.1.4, *LT* is parametrically examined. The results of the experiments show that *LT* by selecting $\omega = 0.08$ can provide a promising result.

Finally, *IMS* was compared with DONG, NPE, SRIE, SRLLI, JED, and LIME similar methods. The results show that the visual quality of enhanced images by *IMS* is similar to LIME method and better than the other methods mentioned. Also, these methods were compared by AMBE, LOE, BRISQUE, NIQE, SSIM and PSNR metrics. In terms of the AMBE metric, *IMS* method is in second place after LIME. According to this, *IMS* can increase the brightness of low-light images more than DONG, NPE, SRIE, SRLLI and JED methods. Also in terms of the LEO metric, enhanced images by *IMS* have better visual quality than all methods of above (except SRIE). In terms of the BRISQUE metric, *IMS* performance was better than all methods mentioned. Moreover, in terms of the NIQE metric, enhanced images by *IMS* look more natural compared to DONG, SRLLI and LIME. In terms of SSIM metric, *IMS* performed better for all test images compared to SRLLI, JED and LIME. Also, in terms of PSNR metric for all test images, *IMS* performance compared to SRLLI and LIME is better. Moreover, computational time of *IMS* compared to all mentioned methods was less. Generally, using *IMS* compare to other methods for low-light images enhancement seems more economical. For this reason, *IMS* can be a good option to increase the performance of computer vision algorithms. In addition, *IMS* can be used independently to enhance low-light images.

References

[1] D. Oneata, J. Revaud, J. Verbeek, and C. Schmid, "Spatio-temporal object detection proposals," 2014, doi: 10.1007/978-3-319-10578-9_48.

[2] A. Krizhevsky, I. Sutskever, and G. E. Hinton, "ImageNet classification with deep convolutional neural networks," 2012, doi: 10.1061/(ASCE)GT.1943-5606.0001284.

[3] K. Zhang, L. Zhang, and M. H. Yang, "Fast Compressive Tracking," *IEEE Trans. Pattern Anal. Mach. Intell.*, 2014, doi: 10.1109/TPAMI.2014.2315808.

[4] Y. Liu, R. R. Martin, L. De Dominicis, and B. Li, "Using retinex for point selection in 3D shape

registration," *Pattern Recognit.*, 2014, doi: 10.1016/j.patcog.2013.12.015.

[5] C. Jung, T. Sun, and L. Jiao, "Eye detection under varying illumination using the retinex theory," *Neurocomputing*, 2013, doi: 10.1016/j.neucom.2013.01.038.

[6] C. Couprie, C. Farabet, L. Najman, and Y. LeCun, "Indoor semantic segmentation using depth information," 2013.

[7] S. Sarkar, V. Venugopalan, K. Reddy, M. Giering, J. Ryde, and N. Jaitly, "Occlusion Edge Detection in RGB-D Frames using Deep Convolutional Networks," 2014, [Online]. Available: http://arxiv.org/abs/1412.7007.

[8] K. G. Lore, A. Akintayo, and S. Sarkar, "LLNet: A deep autoencoder approach to natural low-light image enhancement," *Pattern Recognit.*, 2017, doi: 10.1016/j.patcog.2016.06.008.

[9] W. Wang, X. Wu, X. Yuan, and Z. Gao, "An Experiment-Based Review of Low-Light Image Enhancement Methods," *IEEE Access*. 2020, doi: 10.1109/ACCESS.2020.2992749.

[10] Y. S. Chiu, F. C. Cheng, and S. C. Huang, "Efficient contrast enhancement using adaptive gamma correction and cumulative intensity distribution," 2011, doi: 10.1109/ICSMC.2011.6084119.

[11] S. C. Huang, F. C. Cheng, and Y. S. Chiu, "Efficient contrast enhancement using adaptive gamma correction with weighting distribution," *IEEE Trans. Image Process.*, 2013, doi: 10.1109/TIP.2012.2226047.

[12] Z. Huang, T. Zhang, Q. Li, and H. Fang, "Adaptive gamma correction based on cumulative histogram for enhancing near-infrared images," *Infrared Phys. Technol.*, 2016, doi: 10.1016/j.infrared.2016.11.001.

[13] K. Srinivas and A. K. Bhandari, "Low light image enhancement with adaptive sigmoid transfer function," *IET Image Process.*, vol. 14, no. 4, pp. 668–678, 2020, doi: 10.1049/iet-ipr.2019.0781.

[14] Y. T. Kim, "Contrast enhancement using brightness preserving bi-histogram equalization," *IEEE Trans. Consum. Electron.*, 1997, doi: 10.1109/30.580378.

[15] S. Der Chen and A. R. Ramli, "Minimum mean brightness error bi-histogram equalization in contrast enhancement," *IEEE Trans. Consum. Electron.*, 2003, doi: 10.1109/TCE.2003.1261234.

[16] Q. Wang and R. K. Ward, "Fast image/video contrast enhancement based on weighted thresholded histogram equalization," *IEEE Trans. Consum. Electron.*, 2007, doi: 10.1109/TCE.2007.381756.

[17] T. K. Kim, J. K. Paik, and B. S. Kang, "Contrast enhancement system using spatially adaptive histogram equalization with temporal filtering," *IEEE Trans. Consum. Electron.*, 1998, doi: 10.1109/30.663733.

[18] A. M. Reza, "Realization of the contrast limited adaptive histogram equalization (CLAHE) for real-time image enhancement," *J. VLSI Signal Process. Syst. Signal Image. Video Technol.*, 2004, doi: 10.1023/B:VLSI.0000028532.53893.82.

[19] B. Liu, W. Jin, Y. Chen, C. Liu, and L. Li, "Contrast enhancement using non-overlapped sub-blocks and local histogram projection," *IEEE Trans. Consum. Electron.*, 2011, doi: 10.1109/TCE.2011.5955195.

[20] L. Shen, Z. Yue, F. Feng, Q. Chen, S. Liu, and J. Ma, "MSR-net:Low-light Image Enhancement Using Deep Convolutional Network," 2017, [Online]. Available: http://arxiv.org/abs/1711.02488.

[21] C. Wei, W. Wang, W. Yang, and J. Liu, "Deep retinex decomposition for low-light enhancement," *arXiv*. 2018.

[22] K. Xu, X. Yang, B. Yin, and R. W. H. Lau, "Learning to restore low-light images via decomposition-and-enhancement," 2020, doi: 10.1109/CVPR42600.2020.00235.

[23] D. J. Jobson, Z. U. Rahman, and G. A. Woodell, "Properties and performance of a center/surround retinex," *IEEE Trans. Image Process.*, 1997, doi: 10.1109/83.557356.

[24] D. J. Jobson, Z. U. Rahman, and G. A. Woodell, "A multiscale retinex for bridging the gap between color images and the human observation of scenes," *IEEE Trans. Image Process.*, 1997, doi: 10.1109/83.597272.

[25] X. Guo, Y. Li, and H. Ling, "LIME: Low-light image enhancement via illumination map estimation," *IEEE Trans. Image Process.*, 2017, doi: 10.1109/TIP.2016.2639450.

[26] S. Wang, J. Zheng, H. M. Hu, and B. Li, "Naturalness preserved enhancement algorithm for non-uniform illumination images," *IEEE Trans. Image Process.*, 2013, doi: 10.1109/TIP.2013.2261309.

[27] X. Fu, D. Zeng, Y. Huang, X. P. Zhang, and X. Ding, "A Weighted Variational Model for Simultaneous Reflectance and Illumination Estimation," 2016, doi: 10.1109/CVPR.2016.304.

[28] G. Fu, L. Duan, and C. Xiao, "A Hybrid L2 -LP Variational Model for Single Low-Light Image Enhancement with Bright Channel Prior," 2019, doi: 10.1109/ICIP.2019.8803197.

[29] M. Li, J. Liu, W. Yang, X. Sun, and Z. Guo, "Structure-Revealing Low-Light Image Enhancement Via Robust Retinex Model," *IEEE Trans. Image Process.*, 2018, doi: 10.1109/TIP.2018.2810539.

[30] X. Ren, M. Li, W. H. Cheng, and J. Liu, "Joint Enhancement and Denoising Method via Sequential Decomposition," 2018, doi: 10.1109/ISCAS.2018.8351427.

[31] Y. Chang, C. Jung, P. Ke, H. Song, and J. Hwang, "Automatic Contrast-Limited Adaptive Histogram Equalization with Dual Gamma Correction," *IEEE Access*, 2018, doi: 10.1109/ACCESS.2018.2797872.

[32] M. Veluchamy and B. Subramani, "Image contrast and color enhancement using adaptive gamma correction and histogram equalization," *Optik (Stuttg).*, 2019, doi: 10.1016/j.ijleo.2019.02.054.

[33] C. R. Nithyananda, A. C. Ramachandra, and Preethi, "Review on Histogram Equalization based Image Enhancement Techniques," 2016, doi: 10.1109/ICEEOT.2016.7755145.

[34] M. A. Al Wadud, M. H. Kabir, M. A. A. Dewan, and O. Chae, "A dynamic histogram equalization for image contrast enhancement," *IEEE Trans. Consum. Electron.*, 2007, doi: 10.1109/TCE.2007.381734.

[35] J. Y. Kim, L. S. Kim, and S. H. Hwang, "An advanced contrast enhancement using partially overlapped sub-block histogram equalization," *IEEE Trans. Circuits Syst. Video Technol.*, 2001, doi: 10.1109/76.915354.

[36] N. Kong, "A Literature Review on Histogram Equalization and Its Variations for Digital Image Enhancement," *Int. J. Innov. Manag. Technol.*, 2013, doi: 10.7763/ijimt.2013.v4.426.

[37] D. Parihar, A. Singh, and K. Singh, "Illumination Estimation for Nature Preserving low-light image enhancement," pp. 1–11, 2020.

[38] M. K. Ng and W. Wang, "A Total Variation Model for Retinex," *SIAM J. Imaging Sci.*, 2011, doi: 10.1137/100806588.

[39] R. R. Hussein, Y. I. Hamodi, and R. A. Sabri, "Retinex theory for color image enhancement: A systematic review," *International Journal of Electrical and Computer Engineering*. 2019, doi: 10.11591/ijece.v9i6.pp5560-5569.

[40] J. Yang, X. Jiang, C. Pan, and C. L. Liu, "Enhancement of Low Light Level Images with coupled dictionary learning," 2016, doi: 10.1109/ICPR.2016.7899725.

[41] B. Cai, X. Xu, K. Guo, K. Jia, B. Hu, and D. Tao, "A Joint Intrinsic-Extrinsic Prior Model for Retinex," 2017, doi: 10.1109/ICCV.2017.431.

[42] S. Nocedal, Jorge and Wright, "Numerical optimization," *Springer Sci. \& Bus. Media*, 2006.

[43] Z. Ying, G. Li, and W. Gao, "A bio-inspired multi-exposure fusion framework for low-light image enhancement," *arXiv*. 2017.

[44] A. Mittal, A. K. Moorthy, and A. C. Bovik, "No-reference image quality assessment in the spatial domain," *IEEE Trans. Image Process.*, 2012, doi: 10.1109/TIP.2012.2214050.

[45] A. Mittal, R. Soundararajan, and A. C. Bovik, "Making a 'completely blind' image quality analyzer," *IEEE Signal Process. Lett.*, 2013, doi: 10.1109/LSP.2012.2227726.

[46] Z. Wang, A. C. Bovik, H. R. Sheikh, and E. P. Simoncelli, "Image quality assessment: From error visibility to structural similarity," *IEEE Trans. Image Process.*, 2004, doi: 10.1109/TIP.2003.819861.

[47] Y. H. Shiao, T. J. Chen, K. S. Chuang, C. H. Lin, and C. C. Chuang, "Quality of compressed medical images," *J. Digit. Imaging*, 2007, doi: 10.1007/s10278-007-9013-z.

[48] X. Dong *et al.*, "Fast efficient algorithm for enhancement of low lighting video," 2011, doi: 10.1109/ICME.2011.6012107.